

Supporting information for

**Clinically used drug arsenic trioxide targets XIAP and
overcomes apoptosis resistance in an organoid-based
preclinical cancer model**

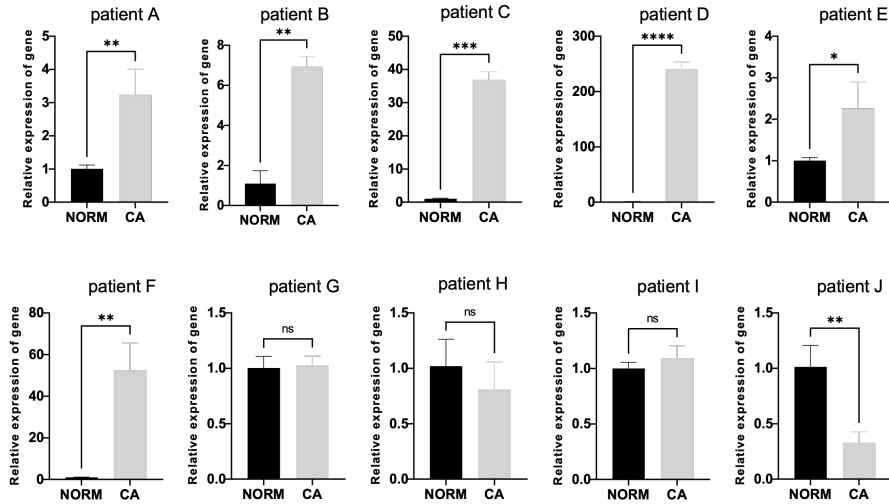


Figure S1 Expression of XIAP in patients diagnosed with colon cancer. The mRNA levels of XIAP in the normal tissue (NORM) and cancerous tissue (CA) were accessed by RT-qPCR assay, which revealed that approximately 60% of the patients' tumors (6 out of 10 patients) exhibited higher expression levels of XIAP. Related to Figure 1.

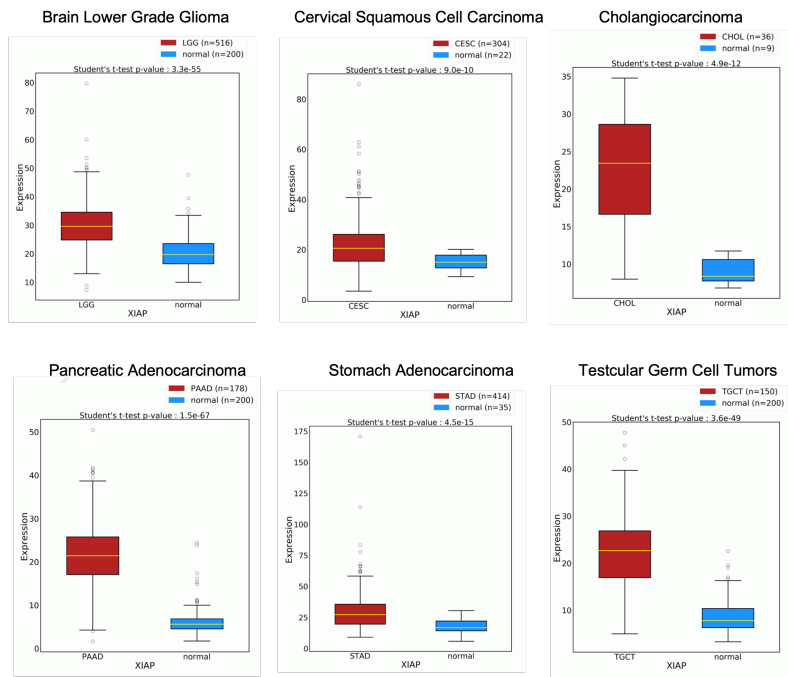


Figure S2 Boxplots to compare RNA expression level of XIAP in tumors vs. normal samples. The OncoDB database was used to investigate XIAP expression patterns in different tumors ¹. Related to Figure 1.

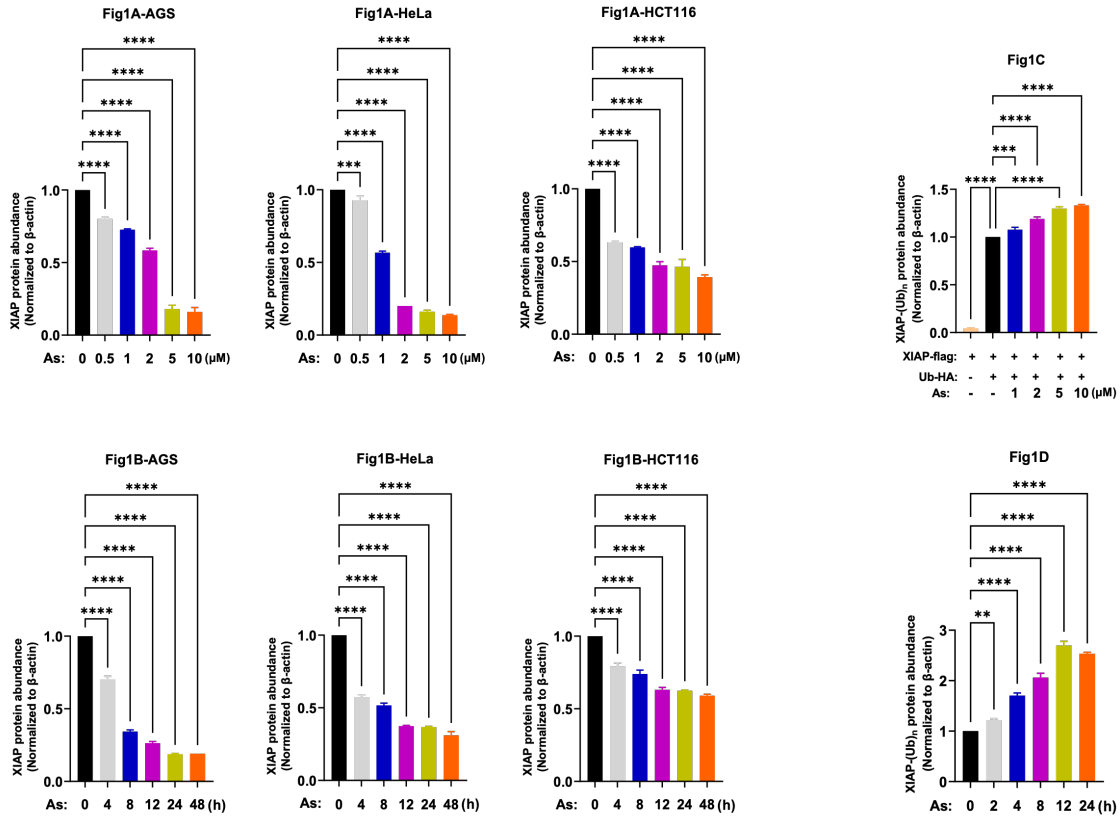


Figure S3 Quantitation of western blots in Figure 1. The intensity of the bands on the blots was evaluated using ImageJ. Related to Figure 1.

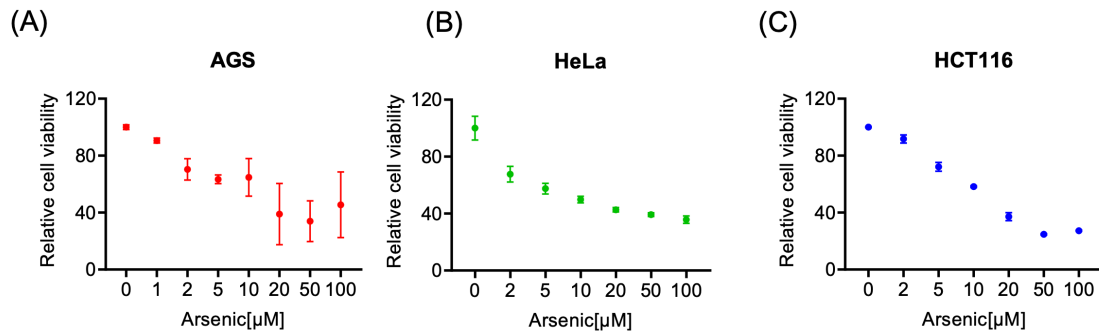


Figure S4 Effect of arsenic treatment on the cell viability of cancer cells. The viability of cancer cells was determined with MTT assay. Related to Figure 1.

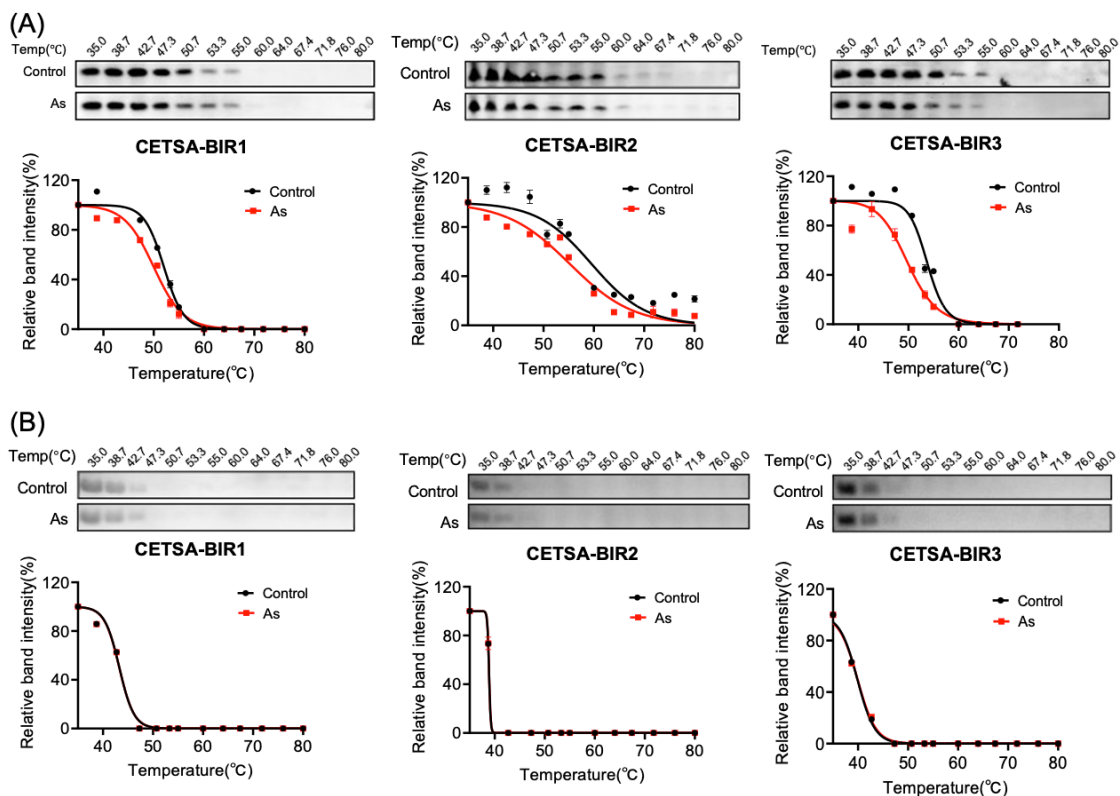


Figure S5 CETSA assay to study the potential As-XIAP interactions. (A) Representative CETSA blot for As-BIR binding in cell. HEK293t cells were pretreated with As for 4 hrs following indicated heat shocks. Soluble XIAP proteins (BIR1, BIR2 or BIR3-Flag) in sample supernatant was revealed by immunoblotting with anti-Flag antibody. The melting temperatures shift (ΔT_m) between treated and control samples is measured based on CETSA melt curves. (B) Representative CETSA gel for As-BIR binding *in vitro*. Apo-BIR1, BIR2 and BIR3 proteins were prepared and NEM was used to block the free Cys residues of these proteins before CETSA assay. The soluble XIAP proteins in the supernatant were analyzed by Coomassie blue staining. Related to Figure 2.

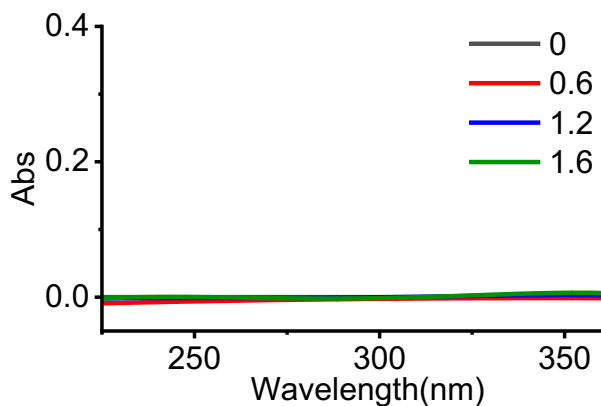


Figure S6 UV absorption spectra of BIR3 upon addition of gradient arsenic as indicated. The sulfhydryl group of Cys in BIR3 was blocked using NEM. Related to Figure 2.

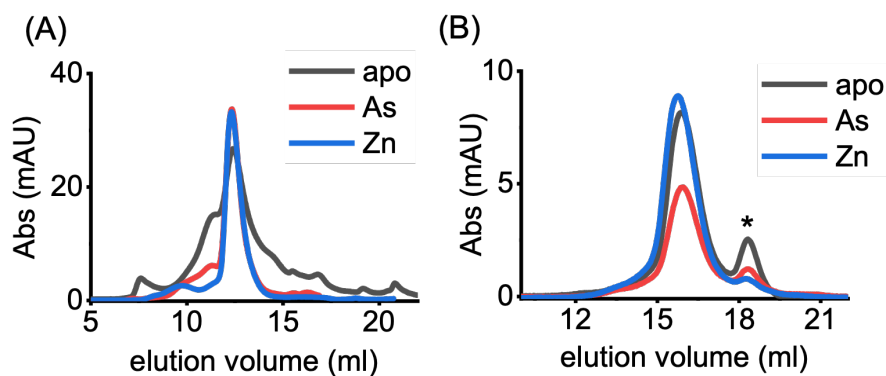


Figure S7 Analytical gel filtration analysis of BIR1/BIR2 domain of XIAP. (A) Profiles of the UV absorbance curve of BIR1 during gel filtration chromatography. Apo-form or Zn/As-bound recombination BIR1(1-150) proteins were prepared and subjected into gel filtration column. (B) Profiles of the UV absorbance curve of BIR2 during gel filtration chromatography. Apo-form or Zn/As-bound recombination BIR2(120-240) proteins were prepared and subjected into gel filtration column. * impurity or fluctuation of the absorbance due to buffer. Related to Figure 3.

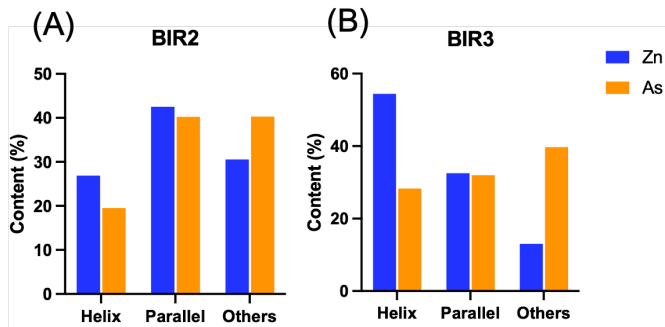


Figure S8 Deconvolution analysis of CD spectra of BIR2 and BIR3 domain proteins. Related to Figure 3.

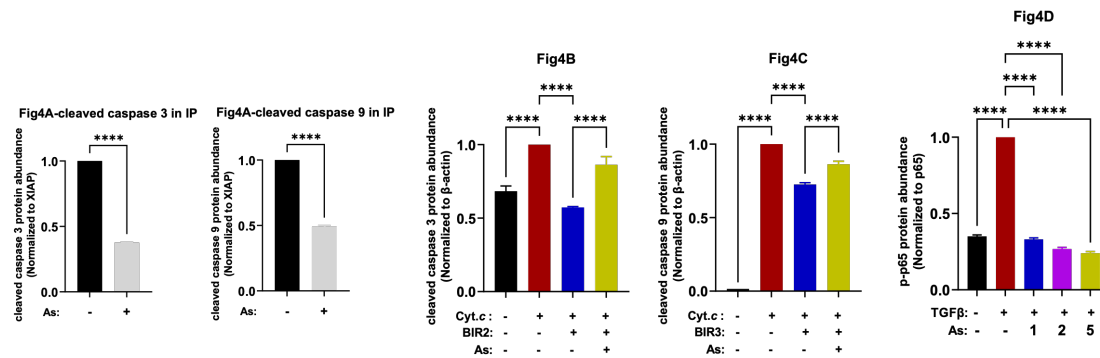


Figure S9 Quantitation of western blots in Figure 4. The intensity of the bands on the blots was evaluated using ImageJ. Related to Figure 4.

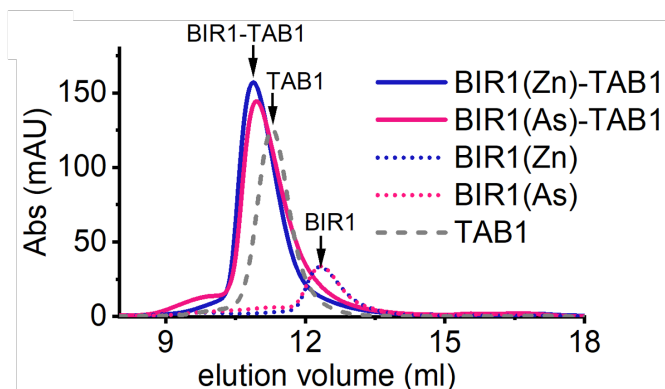


Figure S10 Analytical gel filtration analysis of BIR1-TAB1 complex. Zn- or As-bound recombinant BIR1(1-150) and TAB1(1-370) proteins were pre-incubated and subjected into gel filtration column. Related to Figure 4.

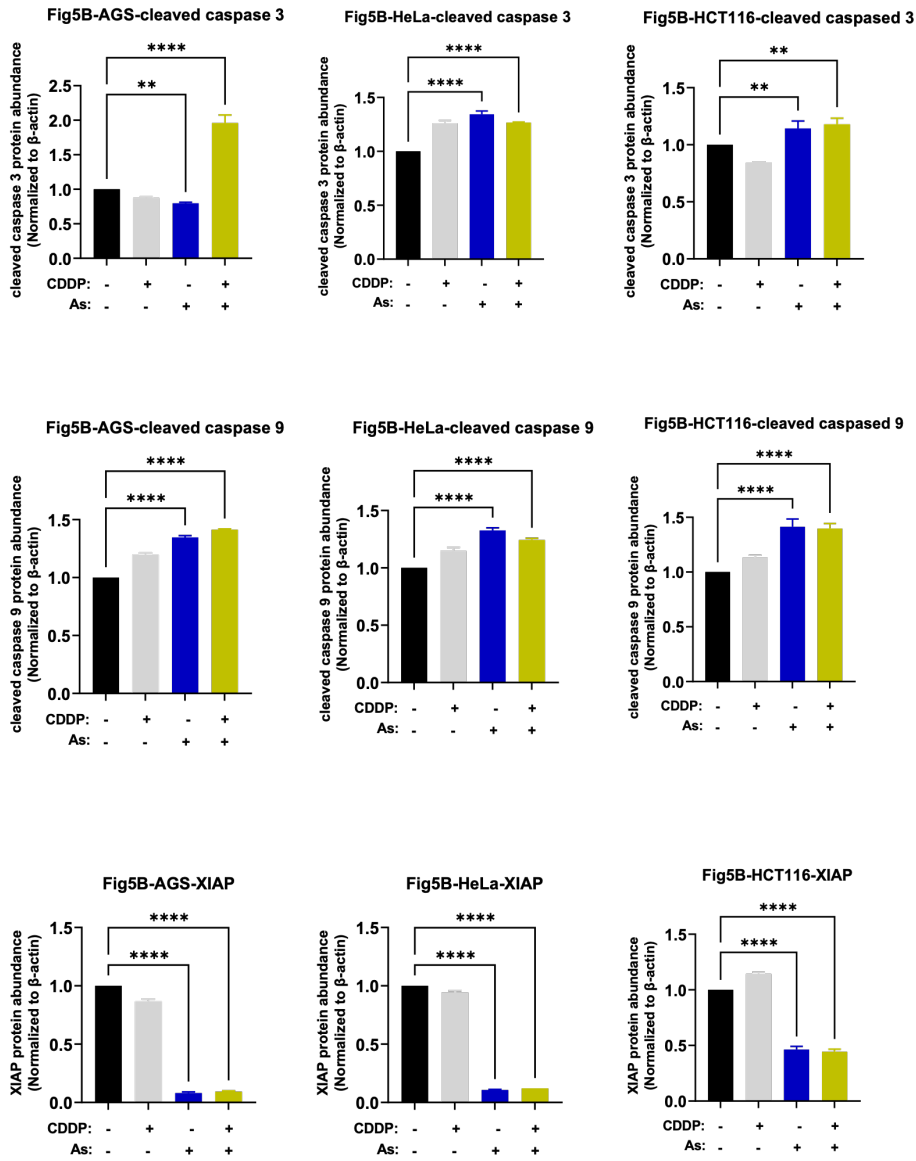


Figure S11 Quantitation of western blots in Figure 5. The intensity of the bands on the blots was evaluated using ImageJ. Related to Figure 5.

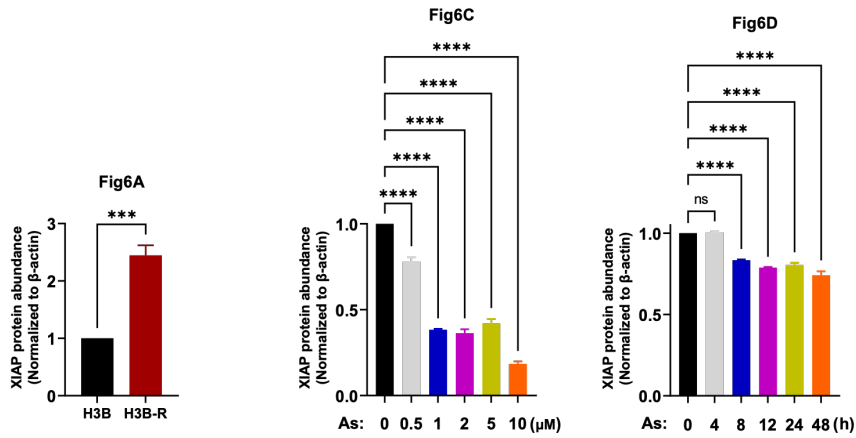


Figure S12 Quantitation of western blots in Figure 6. The intensity of the bands on the blots was evaluated using ImageJ. Related to Figure 6.

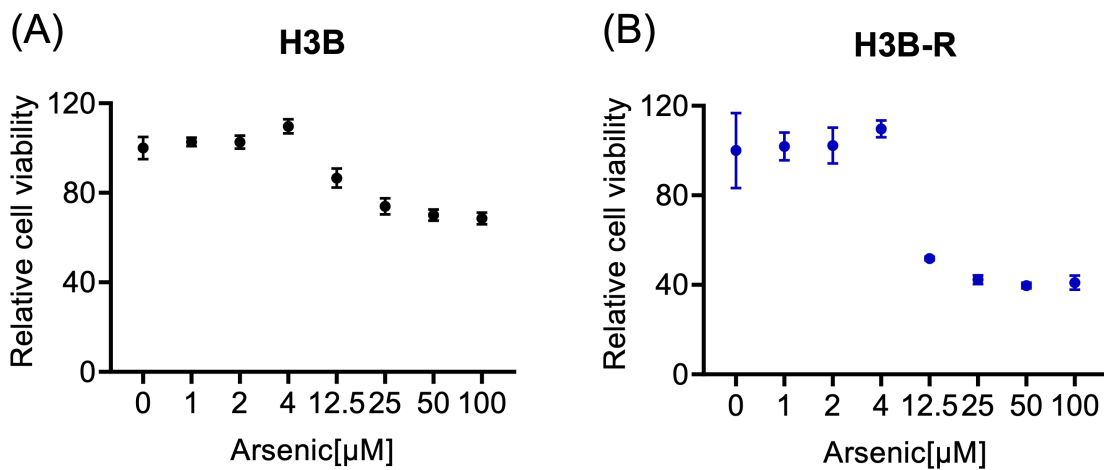


Figure S13 Effect of arsenic treatment on the cell viability of H3B and H3B-R cancer cells. The viability of cancer cells was determined with MTT assay. Related to Figure 6.

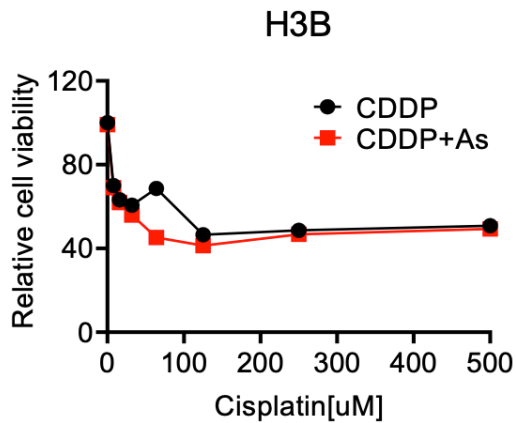


Figure S14 Effect of arsenic/cisplatin treatment on the cell viability of H3B cancer cells. The viability of cancer cells was determined with MTT assay. Related to Figure 6.

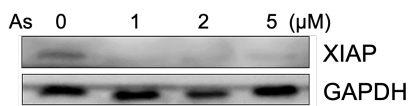


Figure S15 Arsenic induces depletion of XIAP protein in colorectal tumor organoids. Related to Figure 7.

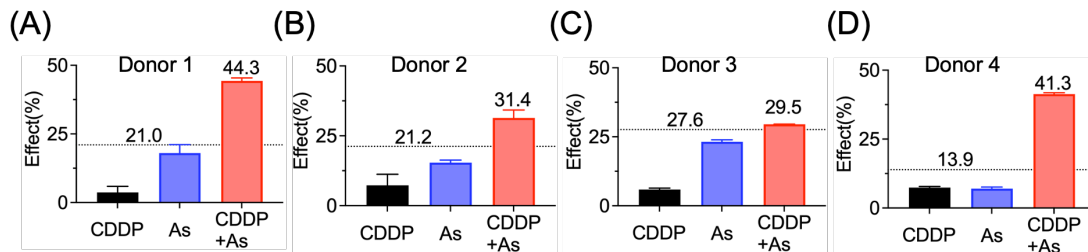


Figure S16 The Bliss Independence Model indicates a synergistic effect for arsenic (1 uM) and Cisplatin (6.25 uM) combination. The Bliss Independence threshold was labeled and shown as dotted line. Related to Figure 7.

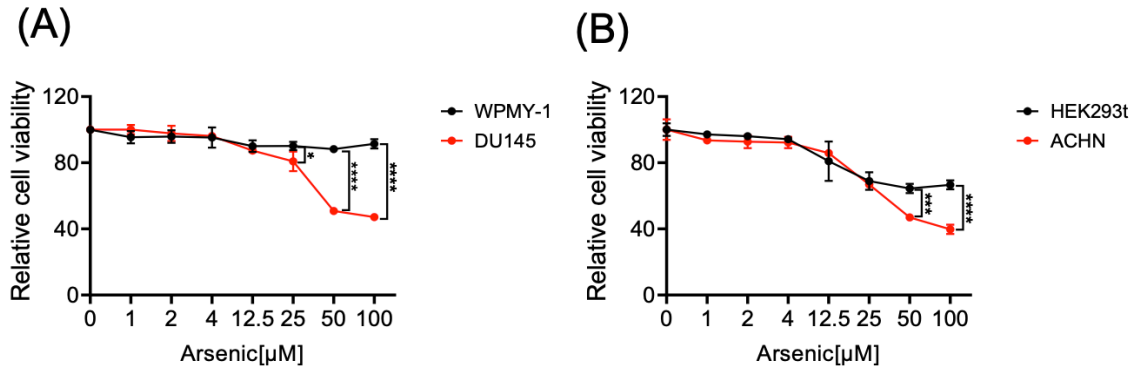


Figure S17 Effect of arsenic treatment on the cell viability in normal cell lines (Black) and cancer cell line (Red). WPMY-1 is a normal prostate cell line, and DU145 is a prostate cancer cell line; HEK293t is a normal kidney cell line, and ACHN is a renal cancer cell line. The cell viability was determined with MTT assay. Cancer cell lines showed reduced viability (depicted in red) compared to normal cell lines (depicted in black). Our results indicate that arsenic exhibits a higher toxicity towards cancer cells.

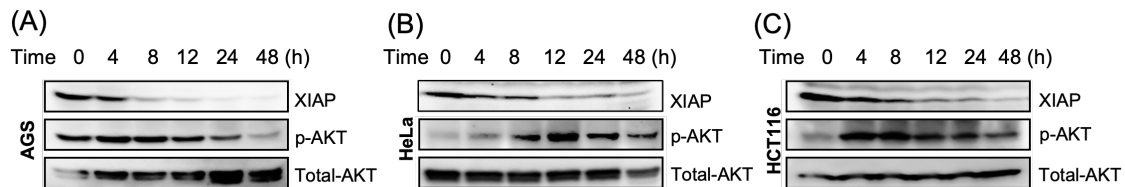


Figure S18 Representative immunoblots of AGS, HeLa and HCT116 cells showing the potential effect of arsenic on Akt pathway. In time-dependent experiments, arsenic (2 μM) was added into the cell cultured medium with the indicated incubation time. Phosphorated and total Akt were revealed by immunoblotting with anti-p-Akt and anti-Akt antibodies respectively.

Figure 1A

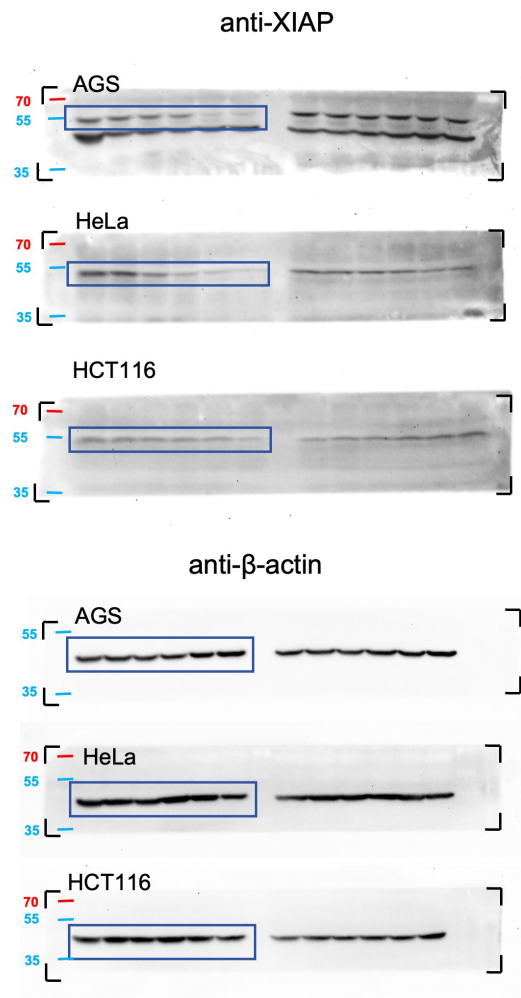


Figure 1B

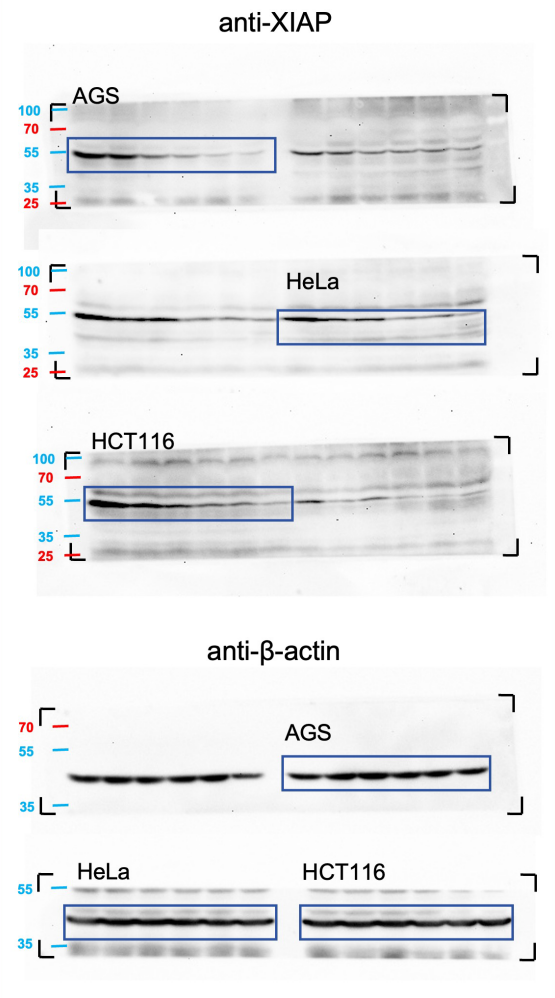


Figure 1C

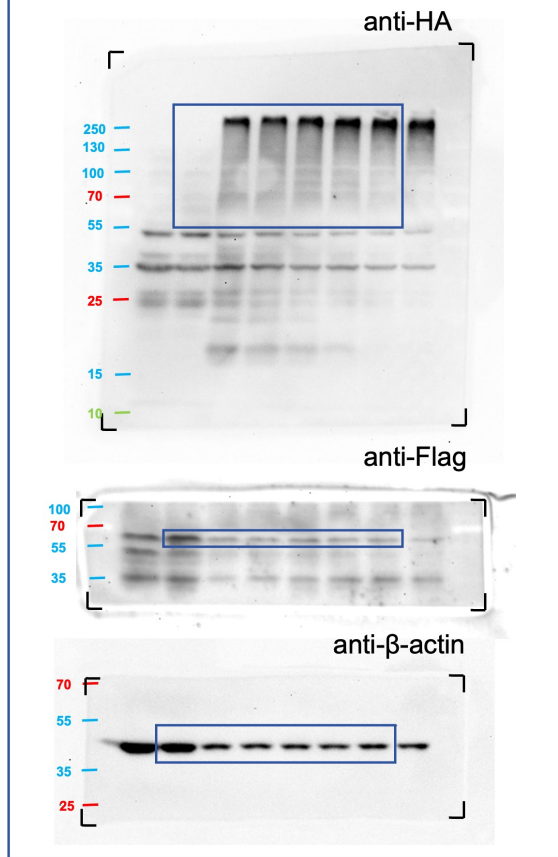


Figure 1D

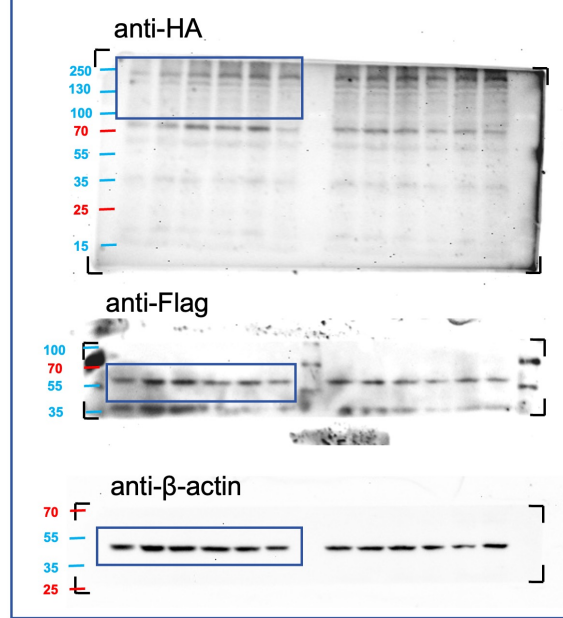


Figure 2A

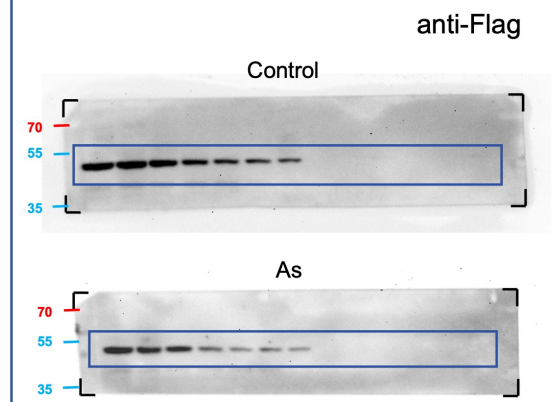


Figure 2B

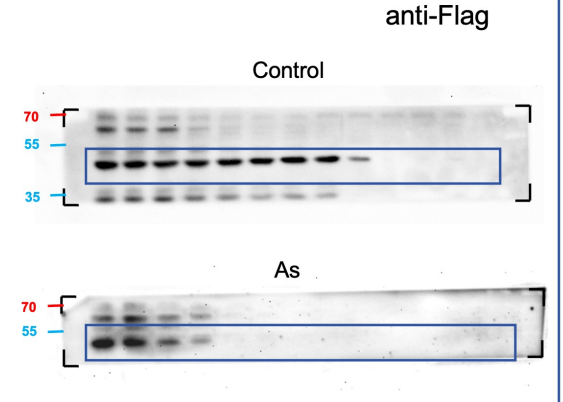


Figure 4A

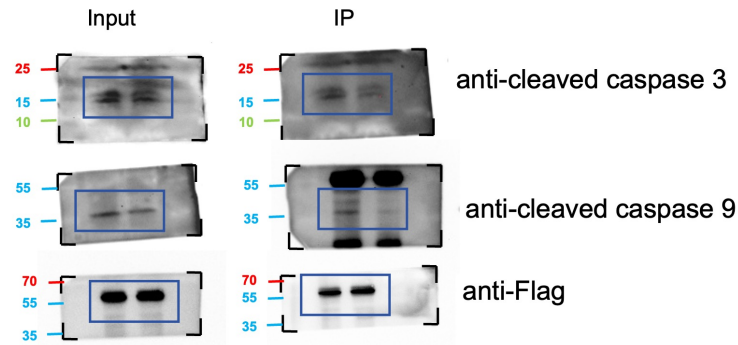


Figure 4B

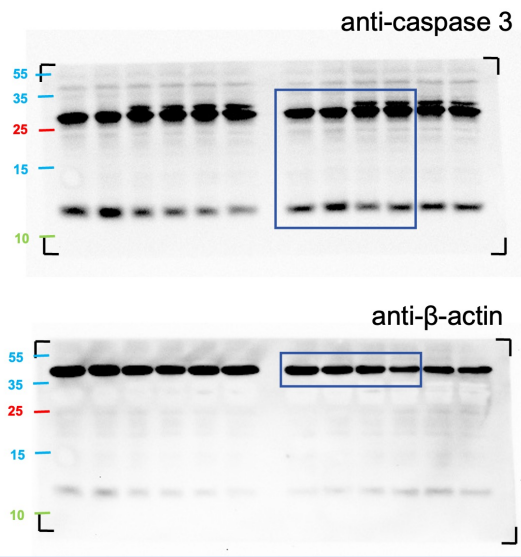


Figure 4C

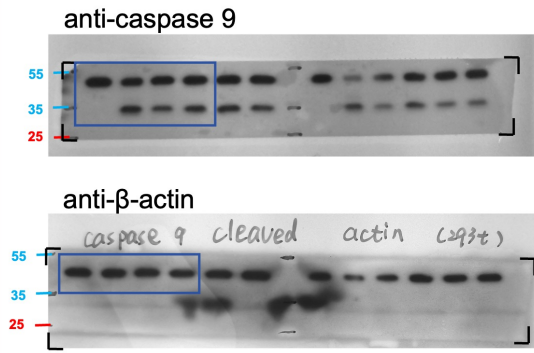


Figure 4D

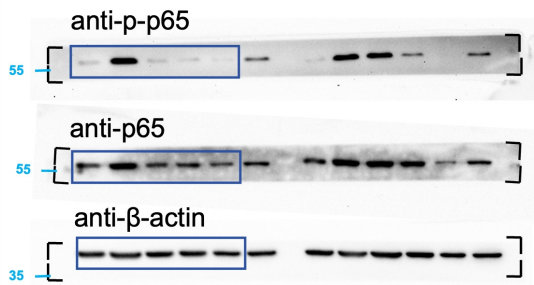


Figure 5B

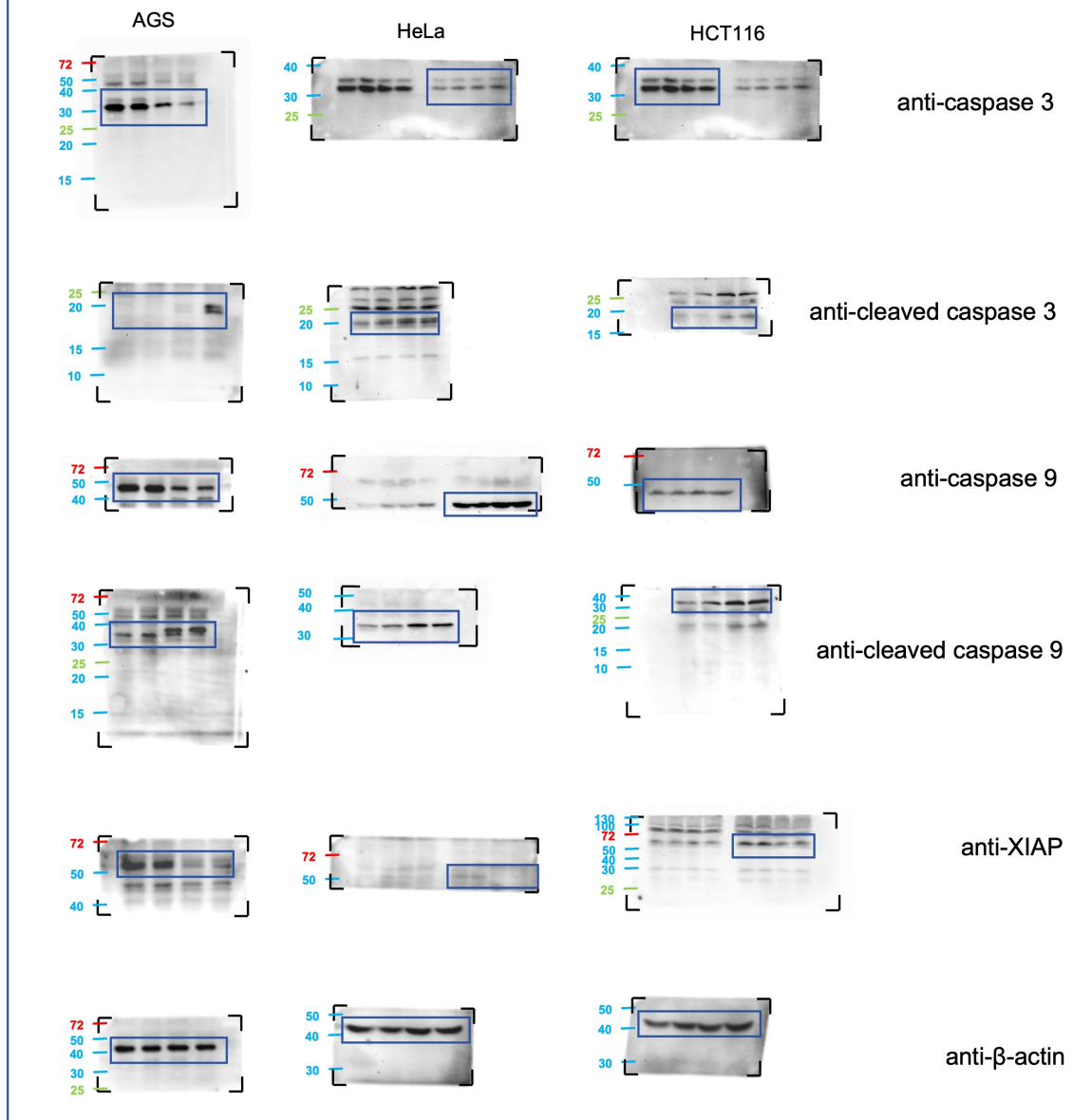
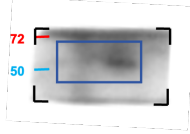
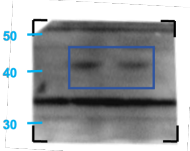


Figure 6A

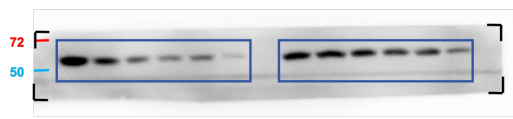


anti-XIAP

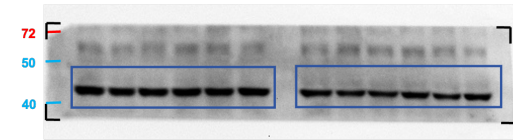


anti-β-actin

Figure 6C-D



anti-XIAP



anti-β-actin

Figure S5A

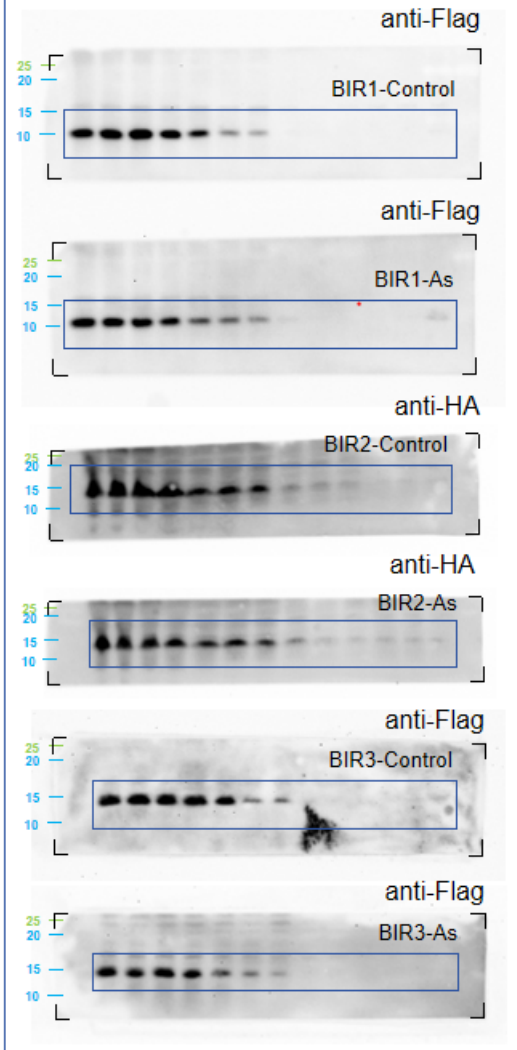


Figure S5B

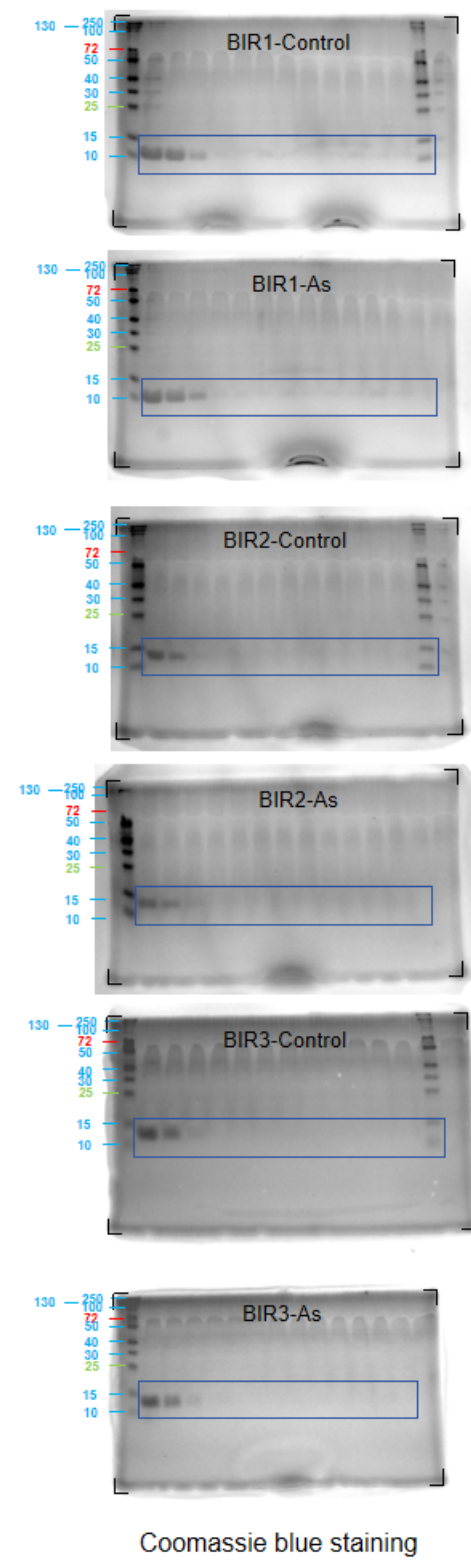


Figure S15

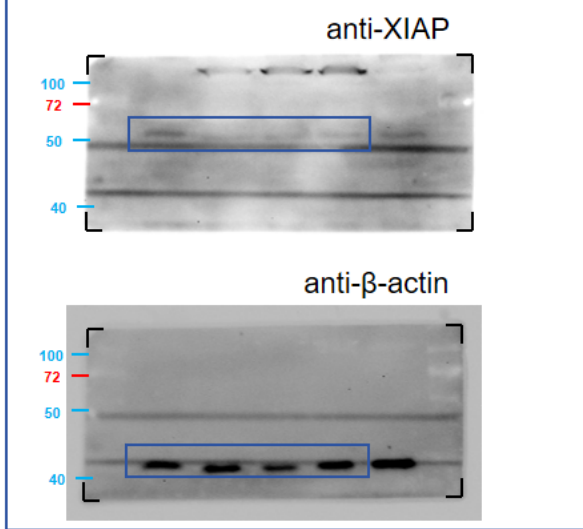
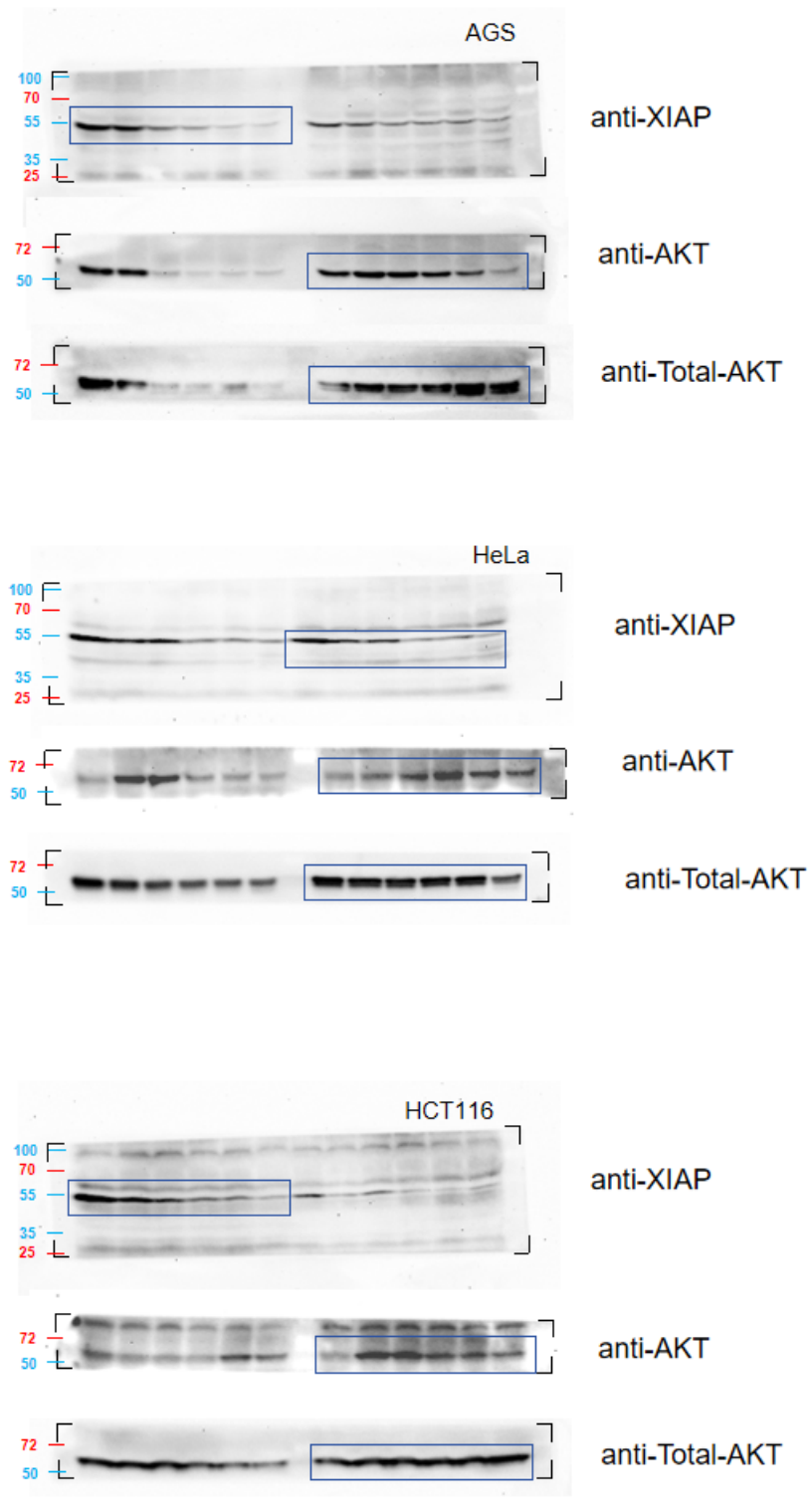


Figure S18



References:

1. G. Tang, M. Cho and X. Wang, OncoDB: an interactive online database for analysis of gene expression and viral infection in cancer, *Nucleic Acids Res*, 2022, **50**, D1334-d1339.